PAPER

Check for updates

Novel protein nanofibril–carbon hybrid adsorbent efficiently removes As(III), As(V) and other toxic elements from synthetic and natural waters in batch and rapid small-scale column tests†

Akram Rahimi,[ab] Sreenath Bolisetty,*[ab] and Stephan J. Hug [iD] *[a]

Novel adsorbents produced from β-lactoglobulin, a low-cost milk protein, have shown a high affinity to inorganic As(III) and As(V). Here, we report an application-oriented investigation of As-removal from synthetic and spiked natural groundwaters with a protein nanofibril carbon composite adsorbent. In batch experiments, removal of both As(V) and As(III) was efficient and not strongly affected by variations in Mg^{2+}, Ca^{2+}, and HCO_3^-, while phosphate exerted a negative influence. 50–500 mg L^{-1} of adsorbent was sufficient to reduce As-concentrations from 50–500 µg L^{-1} to less than 10 µg L^{-1}. Adsorption kinetics were well-described by a second-order rate law. In rapid small scale column tests (RSSCTs) with 1.0 g sieved adsorbent, 100 µg L^{-1} As(III) and As(V) in spiked tap water could be reduced to <1 µg L^{-1} for over 40 000 bed volumes (BVs) and to <10 µg L^{-1} for 50 000–70 000 BVs. Heavy metal ions (Cu, Zn, Pb) were also removed, but not nutrient ions such as Na^+, Mg^{2+}, Ca^{2+}, Cl^-, SO_4^{2-}. With 1000 µg L^{-1} As(III,V) and P (phosphate), As and P were removed to <10 µg L^{-1} over more than 5800 BVs. After regeneration with 10 mM NaOH, 2400 more BVs could be treated. The composites are an alternative to established Fe(III)(hydr) oxide-based adsorbents. Distinct advantages are high efficiencies for removal of As(III) and As(V), low effluent concentrations, and regenerability. The activated carbon carrier can also potentially remove organic compounds and unpleasant odors and tastes.

Water impact

Arsenic contamination in groundwater has been considered as the most serious inorganic contamination in drinking water. The milk protein nanofibril based technology has shown extraordinary results for the removal of both arsenite As(III) and arsenate As(V). In order to implement the novel technology in drinking water treatment plants, many parameters including adsorption capacity, adsorption kinetics and its performance at various water chemistries need to be known. In this manuscript, we report both experimental results and quantitative evaluations on the adsorbent performance in batch and rapid column tests. Our results show that 50 000–70 000 bed volumes of tap water spiked with 100 µg L^{-1} As(III) or As(V) can be treated to below 10 µg L^{-1} As. Together with As, low concentrations of Zn, Cu, Pb and U in the tap water were also greatly reduced, while nutrient cations such as Na, Mg, K, Ca were not affected.

1. Introduction

The health of over 220 million people is still at risk due to the presence of arsenic (As) in drinking water at concentrations above the WHO, EU, US and many national limits of 10 µg L^{-1}, often also above the older and still acceptable limit in some countries of 50 µg L^{-1}.[1-3] There are many established and widely used methods for the removal of arsenic; the most widely applied procedures are precipitation with Fe(II,III) salts and adsorption on Fe(hydr)oxides and Al(hydr)oxides in fixed-bed filters.[4,5] However, new materials are needed for several reasons: (i) each of the established methods has disadvantages under certain conditions (*e.g.* operational complexity, cost, required contact times); (ii) all established methods using Al- or Fe-based precipitation or adsorption require oxidation of As(III) to As(V) for efficient removal; (iii) in many countries, As-limits will be lowered to <10 µg L^{-1} and it is not clear how well the currently applied methods will achieve limits as low as 1 µg L^{-1};[6] (iv) waters with As-concentrations above 10 µg L^{-1} often contain

[a] Eawag, Swiss Federal Institute of Aquatic Science and Technology, CH-8600 Dübendorf, Switzerland. E-mail: stephan.hug@eawag.ch
[b] BluAct Technologies GmbH, Dufauxstrasse 57, CH-8152 Glattpark, Switzerland. E-mail: sreenath@bluact.com
† Electronic supplementary information (ESI) available: Fig. S1: scheme of RSSCT column, Fig. S2: preservation of nutrient ions. See DOI: https://doi.org/10.1039/d2ew00502f

This journal is © The Royal Society of Chemistry 2023

Environ. Sci.: Water Res. Technol., 2023, **9**, 375–385 | 375

Paper

other potentially toxic trace metals[7,8] and organic compounds. New adsorbents that can remove As(III), As(v), and simultaneously other trace elements and organic compounds, without removing nutrient ions such as Ca^{2+} and Mg^{2+}, would be highly advantageous and in demand in many situations.[9]

Protein fibril-based adsorbents as a new class of efficient adsorbents for As and other metals and trace elements have been developed and described first by Bolisetty and Mezzenga.[10,11] These protein fibrils were tested for the removal of arsenic,[12] fluoride,[13] various heavy metals,[14–17] radionuclides[18] and organic contaminants.[19] As-removal has recently been tested field trial in Peru.[20] The general properties and synthesis of the protein fibrils have been described and reviewed by several authors.[21] However, the capacity of the adsorbents and the number of achievable bed volumes (BVs) in filter columns for removal of As(III) and As(v) from contaminated groundwater to levels below the international limit of 10 µg L^{-1}, have not been investigated so far. Here we report an application-oriented laboratory study with various synthetic and natural waters ranging from soft to hard and with different concentrations of Ca^{2+}, Mg^{2+}, HCO_3^-, SO_4^{2-}, H_4SiO_4 and $H_2PO_4^-/HPO_4^{2-}$ in batch experiments and removal of As(III) and As(v) from spiked groundwater in rapid small-scale column tests (RSSCTs). The objective was to quantify the capacity of the new adsorbent for the removal of As from different types of water and to determine the achievable number of bed volumes for the treatment of water with various initial As and phosphate concentrations to the required limit of 10 µg L^{-1}, as well as the removal of other metal ions.

2. Experimental section

2.1. Stock solutions

The following stock solutions were prepared to spike the used waters with As(III), As(v), phosphate, and silicate: 1.00 mg As(v)/ml (208.2 mg $Na_2HAsO_4 \cdot 7H_2O$ in 50 ml H_2O), 1.00 mg As(III)/ml (173.3 g $AsNaO_2$ in 100 ml H_2O), 1.00 mg P/ml (439.4 mg KH_2PO_4 in 100 ml H_2O), and 2.0 mg Si/mL (202.4 mg $Na_2SiO_3 \cdot 9H_2O$ in 10 ml), prepared fresh daily. All chemicals used were analytical grade from Sigma-Aldrich.

2.2. Synthetic ground water, bottled water and local tap water

To probe the influence of various ions occurring in natural waters, experiments were conducted with synthetic hard ground water, medium hard tap water, and very soft mineral water (VOSS). For the experiments, the waters were spiked with various concentrations of As(III), As(v), and phosphate (Table 1). Synthetic groundwater containing 2.5 mM Ca^{2+}, 1.63 mM Mg^{2+}, 9.7 mM HCO_3^-, 1.42 mM Na^+, 0.71 mM Si, 0 or 64.6 µM P and 6.6 µM As was prepared by dissolution of 250 mg L^{-1} $CaCO_3$ and 66 mg L^{-1} MgO with an excess of CO_2 in high purity water (18.2 M Ωcm, Milli-Q® Element, Millipore). To prevent polymerization of added silicate, 10 mL of the alkaline stock solution were rapidly diluted into 1 L CO_2-acidified groundwater (pH < 6.0 with excess dissolved CO_2) with rapid stirring. The pH was subsequently raised to 7.0 by bubbling compressed air through the solution. Phosphate was added from a neutral stock solution (2 ml to 1 L of synthetic water). Finally, the pH was adjusted to 7 by bubbling air, and As(v) and As(III) were added from neutral stock solutions with initial concentrations of 1000 µg ml^{-1}. The concentrations of the ions are listed in Table 1.

2.3. Analysis of influent and effluent water samples

The concentrations of elements in samples of the raw and treated water were measured with inductively-coupled plasma mass spectrometry (ICP-MS, Agilent 7900, Agilent Technologies Inc., CA, USA). IPC Multi-element stock standards (Certipur®, Merk KGaA) were used for the preparation of ICP-MS standards. Detection limits were at

Table 1 Concentrations of major ions in synthetic groundwater, bottled water and tap water

Parameter	Units	Synthetic ground-water	Voss mineral water[a]	Eawag tap water
pH		7.02	5.9–6.0	7.3–7.8
DO	mg L^{-1}	8–9	8–9	8–9
Temp	°C	22–24	22–24	22–24
DOC	mg C L^{-1}	<0.1		1.3
Alkalinity	mmol L^{-1}	9.7	<0.33	3.8–4.0
Cl	mg L^{-1}	<1	3.5	11–20
NO$_3$-N	mg	<0.01	1	
S (as SO$_4$)	mg L^{-1}	<0.01	<5	4.0–6.0
Na	mg L^{-1}	33	3	9.6
Mg	mg L^{-1}	39	0.61	10.5
Ca	mg L^{-1}	100	2.8	69–73
K	mg L^{-1}	2.5	<1	1.5–1.7
P	mg L^{-1}	*(0, 2.0)*	<0.01	<0.01 *(0, 1.0)*
Si	mg L^{-1}	20	1	2.7–2.9
Fe	µg L^{-1}	0	<0.1	<10
As	µg L^{-1}	*(50, 500)*	<0.1 *(50, 500)*	<0.3 *(100, 1000)*

[a] https://www.finewaters.com/bottled-waters-of-the-world/norway/voss All waters were fully aerated and in contact with air. Spiked concentrations of As and P are indicated in parenthesis and slanted font.

least three times lower than the lower concentrations listed or shown in the results section, except for P, for which they were around 20 μg L^{-1}. Standard deviations of ICP-MS measurements were less than ±10% for the lowest and less than ±3% for highest values shown.

2.4. Protein fibrils and granular material preparation

Whey protein isolate was received from Agropur, USA. Activated carbon was purchased from NORIT CABOT. The whey protein fibrils were obtained by heating a 2 wt% whey solution (adjusted to pH 2 with HCl) at 90 °C for 5 h. Granulated media (see Fig. 1) were industrially produced by BluAct Technologies GmbH with their patented technology.[22] The key components of the products are whey protein fibrils and activated carbon. Granulated materials were prepared by absorbing the whey protein fibrils into the activated carbon granules by mixing and drying the carbon granules–amyloid fibrils mixture. The final percentage of protein was 10% (by mass). BluAct granular Mesh Size (U.S sieve) is 12 × 40 and the effective size is 1 (0.4–1.7) mm. For the batch experiments, we used the finer, more easily suspended fraction of particles and for RSSCTs we used 0.25–0.50 mm sieved adsorbent. The measured density of the sieved adsorbent (filled and hand-compressed in the columns) was 1.0 ± 0.05 g cm^{-3}.

2.5. Batch adsorption experiments

Batch adsorption experiments were conducted to determine the amounts of adsorbent needed to remove As to concentrations below 50 μg L^{-1} and 10 μg L^{-1} in different types of water. Increasing amounts of the adsorbent ranging from 1 to 50 mg were dispersed in 50 ml aliquots of the various waters with the same added concentrations of As(v) or As(III) (50 μg L^{-1} or 500 μg L^{-1}). All experiments were conducted in 50–60 mL PP-Sarstedt tubes at pH = 6.9 ± 0.2. The adsorbent and arsenic suspensions were continuously mixed mechanically in an overhead mixer (REAX, Heidolph)
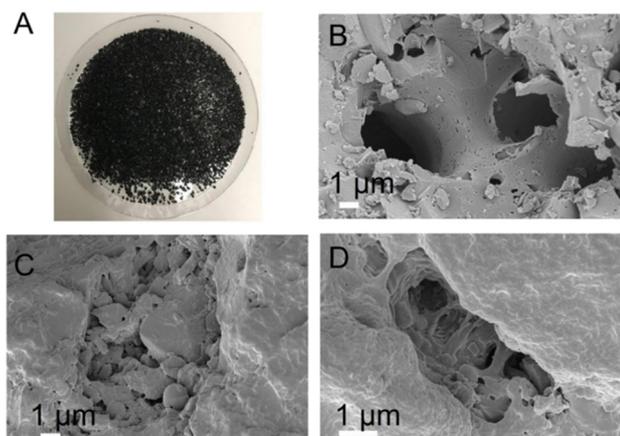

Fig. 1 (A) Granulated protein fibrils activated-carbon composite material (B)–(D) SEM images of the composites of protein fibril granulated material.

at room temperature. 1.0 mL sample volumes were withdrawn after 24 h, filtered (0.2 μm nylon filters) and analyzed with ICP-MS.

2.6. Adsorption kinetics

Different amounts (1 to 50 mg) of the sieved adsorbent were dispersed in 50 ml of synthetic groundwater with spiked concentrations of 50 and 500 μg L^{-1} of As(v) or As(III). The resulting suspensions were shaken mechanically in an overhead mixer at room temperature, and the effect of contact time was evaluated from 2–96 h. After 2, 18, 24, 48, 72, and 96 h, 1.0 ml of the solution was withdrawn, filtered, and analyzed by ICP-MS.

2.7. Rapid small-scale column tests (RSSCTs)

Arsenic removal experiments with spiked tap water in RSSCTs were performed in columns fabricated from 2 ml BD Polypropylene (PP) syringes with 8.66 mm internal diameter and 50 mm length. The active bed length filled with adsorbent was 17 ± 1 mm, see scheme in Fig. S1, ESI.† The columns were operated in upflow mode, with the water entering the syringe through the lower conical Luer connection and leaving through a perforated and shortened polyethylene (PE) syringe plunger. The plunger was pressed against the adsorbent with tight-fitting silicone tubing inserted in the syringe. Layers of 0.1–0.2 mm of compressed cotton fabric at both ends of the syringe were used to hold the adsorbent in place. Each column contained 1.0 + 0.05 g of adsorbent, filling 17 ± 1 mm (1.0 ± 0.06 ml) of the column. In the following calculations, we used an empty BV of 1.0 ml and a density of the adsorbent in the column of 1.0 g cm^{-3}. Column experiments were performed with arsenic spiked tap water with concentrations of main ions similar to groundwaters in As-contaminated regions. Spiked As(v) and As(III) inflow concentrations were 100 μg L^{-1} and 1000 μg L^{-1} As(III,v) and P, see Table 1. Water was pumped through the columns with peristaltic pumps at flow rates of 0.1–2.0 ml min^{-1} in upflow mode (corresponding to loading rates of 0.10–2.03 m h^{-1}), until the outflow concentrations rose to several times above the limit or 10 μg L^{-1} or approached the inflow concentrations. Furthermore, a blank experiment was run with sieved carbon granular materials without protein fibrils. Samples were collected each 12 h or 24 h, diluted in 1% HNO$_3$, and analyzed with ICP-MS. The achievable flow rates after 30 000–50 000 BVs were limited by the maximal pressure of 1.5–2.0 bar, above which the connections between the different tubings started to leak. The flow rates had to be reduced with increasing filtered BVs to keep the inflow pressures in this range.

2.8. Regeneration study

A saturated column after filtering several thousand BVs of tap water with 1000 μg L^{-1} As(v) and 1000 μg L^{-1} P was regenerated by passing 10 mM NaOH solution at a flow rate of 0.25 ml min^{-1} for about 613 ml, followed by gently rinsing with 10–20 BVs DI water to neutralize and remove unabsorbed metal ions. Filtration of tap water with 1000 μg L^{-1} As(v) and 1000 μg L^{-1} P

solution was then resumed to assess the media reusability. After the effluent arsenic concentration exceeded 400 μg L^{-1} again, the column was regenerated a second time with 10 mM NaOH and deionized water.

3. Results

3.1. Removal of dissolved As(III) and As(V) in batch experiments

The removal of dissolved As(III) and As(V) from different types of spiked ground and mineral waters is shown in Fig. 2. The plots show that 50–100 mg L^{-1} adsorbent was sufficient to remove 80% of dissolved As(V) from initially 50 μg As(v)/L (to below 10 μg L^{-1}) in the absence of phosphate. The removal of As(III) and As(V) in the presence of 2 mg P/L (phosphate) required 200 mg L^{-1} or more adsorbent. With initially 500 μg L^{-1} arsenic, 500–1000 mg L^{-1} of adsorbent were needed to lower the dissolved As-concentrations to below 10 μg L^{-1}. The data shows some scatter, most likely due to varying amyloid/carbon ratios in the small amounts (1.0–50 mg) of adsorbent used in the 50 ml suspension experiments. It can be seen that As(V) is removed more efficiently than As(III) and that phosphate exerts a negative influence of As-removal. There was no consistent difference between hard synthetic groundwater (SGW) and soft VOSS mineral water (Table 1), which shows that the influence of Ca^{2+} was minor. Additional studies would be needed to discern the influence of Ca and Si in more detail. With a density of the adsorbent of 1.0 g cm^{-3}, we can estimate that at least 10 000–20 000 BVs of water with 50 μg L^{-1} As(V) can be treated by the addition of adsorbent. In columns, higher numbers of treatable BVs can be expected, as the adsorbent at the inflow of the column is in contact with the high initial concentrations of As, causing a higher loading than at the outflow of the column with the maximum tolerable concentration of 10 μg L^{-1}.
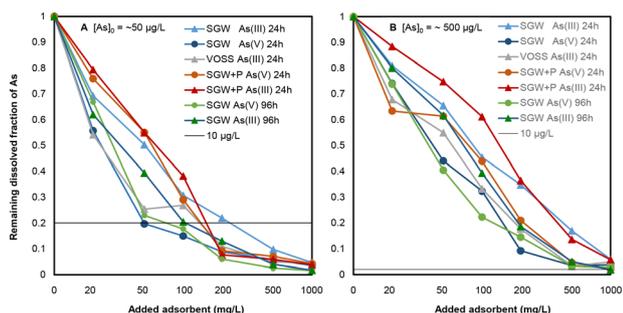

Fig. 2 Removal of dissolved As(v) (circles) and As(III) (triangles) as a function of added adsorbent (in mg L^{-1}, logarithmic scale) in suspensions after 24 h and 96 h. Shown are the fractions of remaining dissolved As after filtration (0.2 μm), with initial concentrations of (A) 45–55 μg L^{-1} and (B) 450–520 μg L^{-1}. The thin lines mark (A) 80% removal and (B) 98% removal to concentrations of 10 μg L^{-1} (WHO, EU and US limit for arsenic). The overall trends are that As(v) removal requires less adsorbent than As(III) removal and that P (phosphate) has a negative effect on both As(III) and As(v)-removal.

3.2. Kinetics of As(III) and As(V) sorption

To determine the necessary times required to reach equilibrium in batch experiments and to obtain estimates for adsorption and desorption rate coefficients in batch and column experiments, kinetic experiments up to 96 h duration were conducted with synthetic groundwater without P (Table 1). Fig. 3 shows measured data (symbols) and kinetic fits (thin lines).

In the kinetics fits, the following equations were used to describe the sorption of dissolved arsenic (As$_{diss}$) to the adsorbent with a certain concentration of initial adsorption sites in the protein fibrils, denoted as [PF≡]$_0$. The concentration of adsorption sites with bound As are denoted as [PF≡As].

With an expected second order rate law, we have the following expressions:

$$d[\text{PF}{\equiv}\text{As}]/dt = -d[\text{As}_{\text{diss}}]/dt = k_{\text{ads}}[\text{As}_{\text{diss}}][\text{PF}{\equiv}] - k_{\text{des}}[\text{PF}{\equiv}\text{As}] \tag{1}$$

at equilibrium:

$$k_{\text{ads}}[\text{As}_{\text{diss}}][\text{PF}{\equiv}] = k_{\text{des}}[\text{PF}{\equiv}\text{As}]$$
$$\text{and } k_{\text{ads}}/k_{\text{des}} = K_{\text{a}} = [\text{PF}{\equiv}\text{As}]/([\text{PF}{\equiv}][\text{As}_{\text{diss}}]) \tag{2}$$

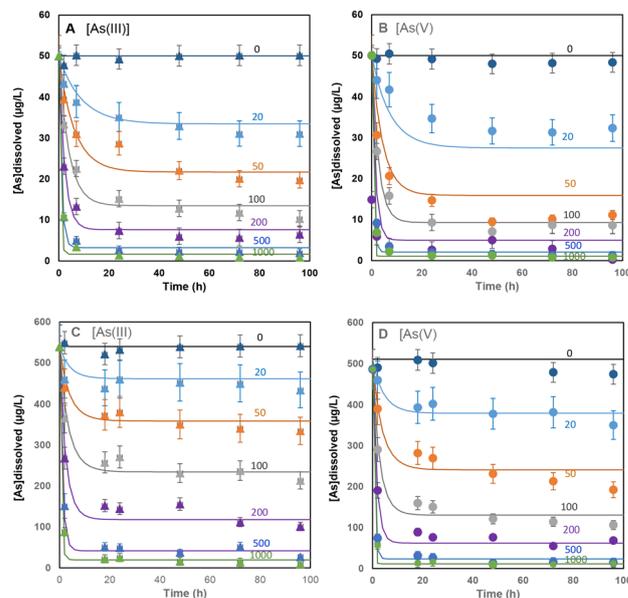**Fig. 3** Kinetics of the removal of As(III) (A and C, triangles) and As(v) (B and D, circles) from synthetic groundwater with 20–1000 mg L^{-1} suspended adsorbent over 96 h. Second-order fits are shown as thin lines with the same colors as the corresponding symbols. The fits are simultaneous fits to all As(III) data with 50 μg L^{-1} and 530 μg L^{-1} initial concentrations, and to all As(v) data with 50 μg L^{-1} and 510 μg L^{-1} initial concentrations. Less than optimal fits to single curves (e.g. to data with 20 mg L^{-1} and 50 mg L^{-1} adsorbents) are thus acceptable, given the overall good fits. For As(III) we obtain $k_{\text{ads}} = 3.4 \times 10^{-4}$ μg^{-1} L h^{-1}, $k_{\text{des}} = 6.4 \times 10^{-2}$ h^{-1}, $K_{\text{ads}} = 5.2 \times 10^{-3}$ μg^{-1} L, $C_{\text{ads,max}} = 5.6$ μg mg^{-1}, for As(v) $k_{\text{ads}} = 3.0 \times 10^{-4}$ μg^{-1} L h^{-1}, $k_{\text{des}} = 6.8 \times 10^{-2}$ h^{-1}, $K_{\text{ads}} = 4.4 \times 10^{-3}$ μg^{-1} L, $C_{\text{ads,max}} = 10.5$ μg mg^{-1}.

With $[PF\equiv] + [PF\equiv As] = [PF\equiv]_0$ (total number of adsorption sites)

$$[PF\equiv As] = [PF\equiv]_0 K_{ads}[As_{diss}]/(1 + K_{ads}[As_{diss}])$$

$$[PF\equiv As] = [PF\equiv]_0 \frac{K_{ads}[As_{diss}]}{1 + K_{ads}[As_{diss}]} \quad (3)$$

This is a Langmuir adsorption isotherm expression, with a single type of adsorption site.

With $[PF\equiv As] = [As_{ads}]$, $[PF\equiv]_0 = C_{ads, max}$

$$[As]_{ads} = [C]_{ads, max} \frac{K_{ads}[As_{diss}]}{1 + K_{ads}[As_{diss}]} \quad (4)$$

As seen in Fig. 3A and C, the second-order rate law describes the measured adsorption kinetics of the As(III) data well. The fits are simultaneous fits to all data with 50 µg L^{-1} and 530 µg L^{-1} starting concentrations, each with 6 different amounts of added adsorbent and a total of 72 data points. The same applies to the fits with As(v) in Fig. 3B and D, except for larger deviations in the data with the lowest amount of added adsorbent (20 mg L^{-1} and 50 mg L^{-1}) and with the 50 µg L^{-1} starting concentrations.

In column experiments with 1 kg adsorbent per liter, we have a large excess of sorption sites over $[As_{diss}]$ and can consider their concentration as constant at certain loadings of the sorbent. Applying pseudo-first order kinetics and rate coefficients (k'_{ads}) for the decrease of $[As_{diss}]$, we can calculate times ($t_1/100$) at which 99% of initially present dissolved is adsorbed. With initially no surface sites occupied with As: for As(III): $k'_{ads} = (1 \times 10^6$ mg L$^{-1} \times 5.6$ µg mg^{-1}) $\times 3.4 \times 10^{-4}$ µg^{-1} L h$^{-1} = 1904$ h^{-1} (0.54 s^{-1}) and $t_1/100 = \ln(100)/k'_{ads} = 8.5$ s. For As(v) we obtain $t_1/100 = 5.3$ s.

If we assume that sorption is mostly determined by the kinetics of the sorption reactions in the protein layers coated on the active charcoal, rather than by film diffusion onto the layers, they will not be strongly dependent on the flow velocities around the particles and should be similar in the batch suspension and in the fixed bed column experiments. We can thus estimate that empty bed contact times (EBCT) in the RSSCT columns of 20–180 s should be sufficient to reach equilibrium between dissolved and adsorbed arsenic along the length of the column.

3.3. Equilibrium adsorption isotherms

Approximate Langmuir and Freundlich adsorption isotherms (Fig. 4A and B) were derived from the last time points from various batch adsorption experiments (Fig. 2A, B and 3A–D) with synthetic groundwater. We consider these adsorption isotherms as "approximate" because there was a considerable amount of scatter in the data, which, as mentioned above, is probably due to heterogeneities in the amyloid/carbon ratio in the small amounts of adsorbent used in the suspension experiments (1–50 mg/50 ml). The objective here was not to obtain well-constrained adsorption isotherms, but estimates for the design of the following RSSCT column experiments.
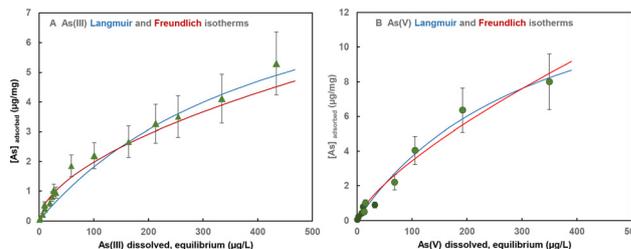

Fig. 4 Adsorption isotherms for As(III) (A, triangles) and for As(v) (B, circles) in synthetic groundwater at close to equilibrium after 72–96 h reaction time. For As(III) we obtain $K_{ads} = 5.5 \times 10^{-3}$ µg^{-1} L, $C_{ads,max} = 6.3$ µg mg^{-1}, and for As(v) $K_{ads} = 2.9 \times 10^{-3}$ µg^{-1} L, $C_{ads,max} = 16.2$ µg mg^{-1}. Error bars ± 20% (average of calculated errors from 3% standard deviations in measured initial and final concentrations and mass of adsorbent).

Both Langmuir and Freundlich isotherms provide acceptable fits to the measured adsorption data (Table 2). Langmuir isotherms give a maximum adsorption capacity and the C_{max} and K_{ads} values can be compared to those obtained from the kinetic fits. The values obtained from the kinetic fits and the adsorption isotherms agree to within ±30%, which was sufficient for estimating the number of achievable BVs for the treatment of water with 100 µg L^{-1} to around 40 000 BVs for As(v) and As(III) to around 20 000 BVs. These estimates are based on the assumption that most of the adsorbent over the length of the column will reach equilibrium with the inflow concentration of 100 µg L^{-1} before the front of high concentrations reaches the outlet and the effluent concentrations start to rise above the limit of 10 µg L^{-1}.

3.4. Rapid small-scale column tests (RSSCTs) with tap water spiked with 100 µg L^{-1} As(v) and As(III)

The results of RSSCTs with tap water spiked with 100 µg L^{-1} As(III) and As(v) are shown in Fig. 5. Flow rates at the start of the experiments were 1.5–2.0 ml min^{-1}, corresponding to 1.5–2.0 BVs per minute and empty bed contact times (EBCT) of 0.5–0.67 min. With increasing BVs, the flow rates had to be reduced due to increasing necessary pressures to maintain the flow rates. Our set-up with peristaltic pumps and PE- and silicon tubing connections limited pressures to 1.0–1.2 bars. Rising flow resistance is common in RSSCTs and is caused by compacting of particles in the filter media due to partial disintegration of particles. Smaller particles occupy pore space, which leads to increased hydraulic resistance. Flow rates after 30 000 BVs in our columns were typically 0.5 ml min^{-1} (ECBT = 2 min) and down to 0.2 ml min^{-1} (ECPBT = 5 min) after 50 000 BVs. Fig. 5A shows the inflow and outflow concentrations with As(III) up to 60 000 BVs and with As(v) up to 90 000 BVs. Treatment of tap water with initially 100 µg L^{-1} As(III) or As(v) to outflow concentrations below 10 µg L^{-1} was possible until 65 000 BVs. Fig. 5B, with concentrations plotted on a logarithmic scale, shows that outflow As-concentrations were extremely low (<1 µg L^{-1}) for over 40 000 BVs, both for As(III) and As(v).

This journal is © The Royal Society of Chemistry 2023

Environ. Sci.: Water Res. Technol., 2023, **9**, 375–385 | **379**

Table 2 Rate coefficients for adsorption and desorption, equilibrium adsorption constants from Langmuir fits, parameters for Freundlich fits

Langmuir fits	k_{ads} μg^{-1} L h^{-1}	k_{des} h^{-1}	K_{ads} μg^{-1} L	C_{max} μg mg^{-1}	SS$_r$	$C_{10\ \mu g\ L^{-1}}$ μg^{-1} mg^{-1}	$C_{100\ \mu g\ L^{-1}}$ μg^{-1} mg^{-1}	$C_{1000\ \mu g\ L^{-1}}$ μg^{-1} mg^{-1}
As(III) kinetic	3.4×10^{-4}	6.4×10^{-2}	5.2×10^{-3}	5.6				
As(v) kinetic	3.0×10^{-4}	6.8×10^{-2}	4.4×10^{-3}	10.5		0.44	3.2	8.5
As(III) equilib.			5.5×10^{-3}	6.3	1.75			
As(v) equilib.			2.9×10^{-3}	16.2	1.06	0.65	3.4	12.2
Freundlich fits			*1/n*	*A*				
As(III)			*0.147*	*1.77*	*1.60*			
As(v)			*0.124*	*1.39*	*1.90*			

For the definitions of k_{ads}, k_{des} and K_{ads} see eqn (1)–(4), for k_{Th} and q see eqn (5). $C_{10\ \mu g\ L^{-1}}$, $C_{100\ \mu g\ L^{-1}}$ and $C_{1000\ \mu g\ L^{-1}}$ are the sorption capacities at 10, 100 and 1000 μg L^{-1} equilibrium concentrations (see Discussion section). SS$_r$ are the sums of squared residuals (differences) between data and fits.
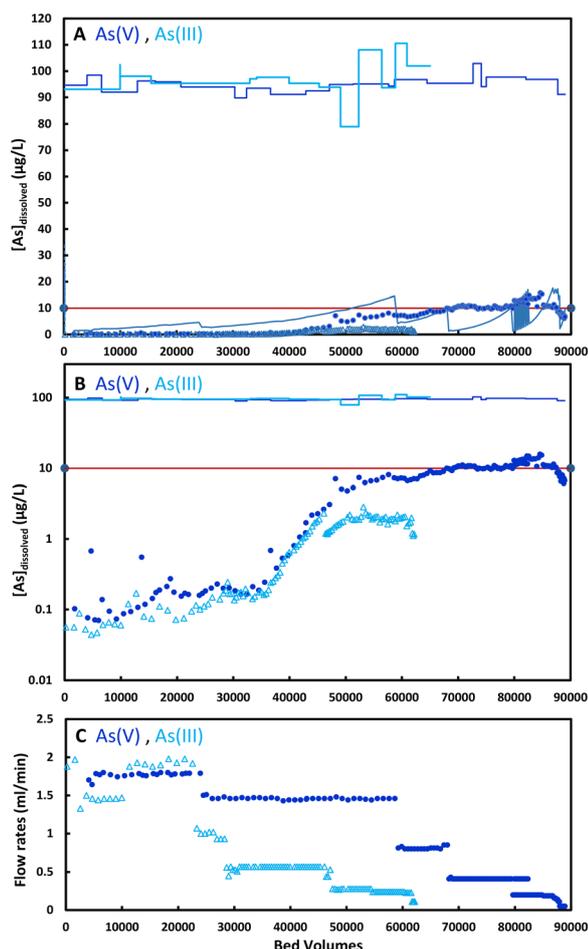

Fig. 5 Rapid small scale column tests (RSSCTs) with tap water spiked with 100 μg L^{-1} As(v) (dark blue circles) or As(III) (light blue triangles). Inflow concentrations (lines) and outflow concentrations (symbols) on a linear scale (A) and on a logarithmic scale (B). The lower blue line in (A) shows the fitted breakthrough curve calculated with the Thomas model for As(v). As(v) and As(III) outflow concentrations were below 10 μg L^{-1} (red line) for up to 68 000 BVs (68 L) and extremely low (<1 μg L^{-1}) for the first 40 000 BVs. (C) Shows the flow rates during the filtration. Flow rates of 1.5 ml min^{-1} correspond to loading rates of 1.53 m h^{-1}.

3.5. Removal of high concentrations of As in the presence of phosphate

People in many of the worst affected regions, particularly in Bangladesh, rely on groundwater with high concentrations of As(III) and phosphate. In most established methods for As-removal, P (phosphate) lowers the removal of both As(III) and As(v), because phosphate outcompetes As(III) and competes with As(v) for adsorption on adsorption sites in Al- and Fe-precipitates and on the surface of pre-formed Al- and Fe(III) (hydr)oxide adsorbents. To test for selectivity of the β-lactoglobulin amyloid fibrils for arsenite and arsenate over phosphate, we conducted experiments with high concentrations of both As(III) and P and As(v) and P. Concentrations of As and P in this range occur in natural groundwaters in Bangladesh, Cambodia and other countries.

Fig. 6 shows inflow and outflow concentrations of tap water containing 1000 μg L^{-1} P (added as KH$_2$PO$_4$) and of As(III) or As(v). Remarkably, both As(III) and As(v) were removed from 1000 μg L^{-1} to below 10 μg L^{-1} (99% removal) up to 5800–6000 BVs in the presence of 1000 μg L^{-1} P. The logarithmic plots in Fig. 6B show that up to 4000 BVs, removal is over 99.9% to <1 μg L^{-1} As. The limit of detection for P in our ICP-MS measurements was 20 μg L^{-1} and we could thus not determine when P outflow concentration exceeded 10 μg L^{-1}. However, we see that P was removed similarly to As. The breakthrough curves in Fig. 6A and B for phosphate occur earlier and increase more steeply than for As(III) and As(v), which shows that there is a moderate selectivity for As over P.

3.6. Regeneration of adsorbent with 10 mM NaOH

After the almost complete breakthrough of P and As(v) at 15 300 BC (Fig. 6B), the column was regenerated with 613 BVs of 10 mM NaOH. Since the empty bed volume was 1.0 ml, this amounted to 613 ml. Outflow concentrations during regeneration were initially 15.5 mg L^{-1} and dropped to 2.1 mg L^{-1} at the end of the regeneration. The sum of As(v) released was approximately 2.9 mg (an exact calculation was not possible for lack of sufficiently frequent measurements). Following regeneration, an additional 2430 BVs could be treated again to below 10 μg L^{-1}. A second regeneration after
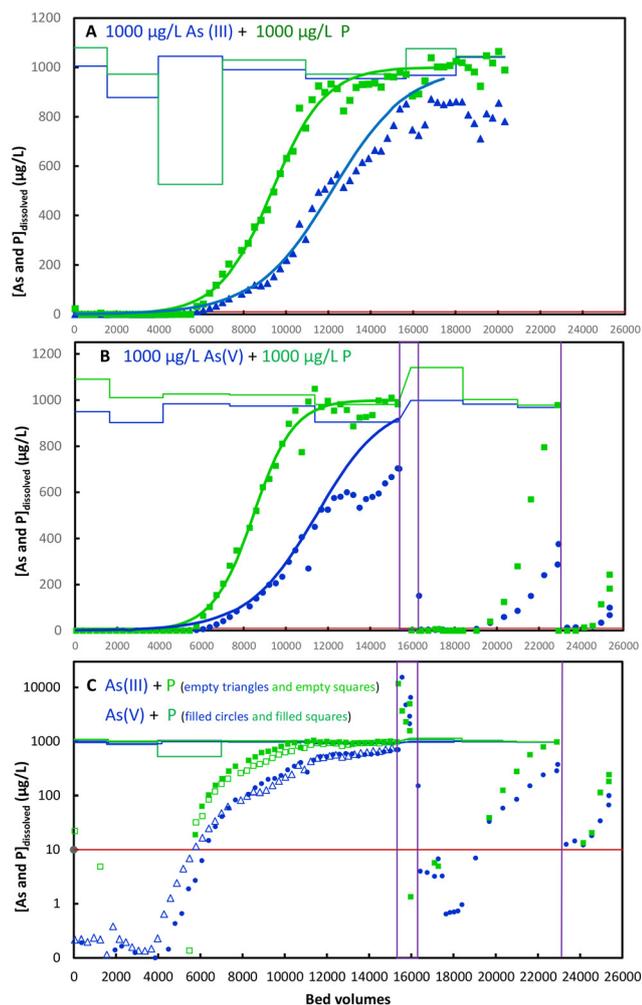
Fig. 6 RSSCTs with tap water spiked with 1000 μg L^{-1} As(III) or As(V) and 1000 μg L^{-1} P (phosphate). (A) and (B) linear scale, (C) logarithmic scale. Inflow concentrations are shown as thin lines, outflow concentration as symbols (colors as indicated in the plots). The thicker green and blue lines are fits with the Thomas model. Outflow concentrations were below 10 μg L^{-1} for up to 5800 BVs (5.8 L) for As(III) and 6000 BVs (6.0 L) for As(V) and extremely low (<1 μg L^{-1}) for the first 4000 BVs. After regeneration of the As(V) column with 10 mM NaOH (purple box), outflow concentrations were again below 10 μg L^{-1} for another 2430 BVs. After a second regeneration (purple line), more than 90–99% of As(V) was still removed for about 2000 BVs but not to below 10 μg L^{-1}. P was removed similarly to As(III) and As(V), but increased more rapidly after 6000 BVs. Flow rates for As(III) were 0.40–0.44 ml min^{-1}, for As(V) 0.42–045 ml min^{-1}, except from BV 15 380–18 400 and 22 900–25 400, where they were 0.25–0.28 ml min^{-1} for As(V).

22 888 BVs did not achieve outflow concentration below 10 μg L^{-1}, but 1612 more BVs could be treated to below 50 μg L^{-1}. Partial regeneration of the adsorbent with 10 mM NaOH is thus possible, extending the usable range of 5750 BVs to 5750 + 2430 = 8180 BVs.

3.7. Removal of Cu, Zn, Pb and U

Unwanted elements Cu(II), Zn(II) and particularly toxic Pb(II) in the tap water were removed to very low concentrations, as
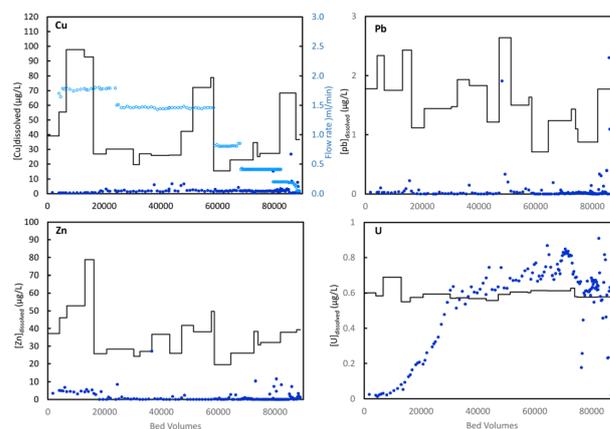

Fig. 7 Removal of Cu, Pb, Zn, U from the As(V)-spiked tap water (results for As shown in Fig. 5). Inflow concentrations (with variations in the tap water) are shown as black lines, column outflow concentration as blue symbols.

shown in Fig. 7. The elements were present in the tap water at concentrations below the WHO limits and European Union parametric values (2 mg L^{-1} for Cu, 3 mg L^{-1} for Cu, 10 μg L^{-1} for Pb). Even at these low concentrations, Cu, Zn and Pb were efficiently removed (>95%) over more than 70 000 BVs to concentrations far below recommended values. In contrast, uranium (present as U(VI) in oxic water) was removed to over 90% only until *ca.* 1200 BVs and complete break-through was observed 30 000 BVs. Since the WHO, EU and US limits for U in drinking water are 30 μg L^{-1}, removal of U simultaneous to As-removal is often not required. The selectivity for As over U can be an advantage in practice, because adsorbents that accumulate U can reach a level of radioactivity that requires disposal in special and costly waste deposits.

3.8. Preservation of nutrient ions in drinking water

Inflow and outflow concentrations of usually present and wanted elements in drinking water are shown in Fig. S2, ESI.† The columns did not remove Na$^+$, K$^+$, Mg^{2+}, Ca^{2+}, Sr^{2+}, Ba^{2+}, Si, Cl$^-$, SO$_4^{2-}$. There was some minimal retention of Ca^{2+}, Ba^{2+} and Si (H$_4$SiO$_4$ at neutral pH) at the start of the filtration and when the water in the inflow reservoir or the flow rates changed. Except for occasional temporary reductions in the concentration of Ca^{2+} and Ba^{2+} (which might be due to precipitation as carbonates), there was no significant overall removal of these elements.

4. Discussion

4.1. Adsorption capacities in batch experiments and columns

The adsorption capacities of adsorbents are determined by equilibrium adsorption isotherms (such as Langmuir or Freundlich isotherms), as shown in Fig. 4 for this adsorbent. The average adsorption capacity in a column somewhere is between the adsorption capacities at the inflow and the outflow concentrations, dependent on how equilibrium in each segment of the columns is reached and how sharp the

This journal is © The Royal Society of Chemistry 2023

Environ. Sci.: Water Res. Technol., 2023, **9**, 375–385 | 381

front of high concentrations moves along the column until outflow concentrations exceed the accepted limit (10 μg L^{-1} for As). Experiments with submerged microfiltration units by Usman et al.[23] studied the adsorption capacities of low-cost micro-sized iron oxyhydroxide-based adsorbents for As(v). The adsorption capacities at 10 μg L^{-1} As(v) were 0.95–1.04 μg mg^{-1}. In our study, we obtained 0.44 μg mg^{-1} at 10 μg L^{-1} and 3.2 μg mg^{-1} at 100 μg L^{-1} (Table 2) for synthetic groundwater. In a column with ideal homogeneous flow conditions and sufficient contact time for the establishment of adsorption equilibrium within each segment of the column, a front with inflow concentrations moves slowly along the column, so that before the breakthrough, most of the length of the absorbent in the column is in equilibrium with the inflow concentration. In larger columns, equilibrium conditions are often not reached within practical contact times, particularly in columns in which adsorption kinetics are limited by slow intra-particle diffusion. Under these conditions, breakthrough curves become broad and achievable BVs are determined by weighted averages between adsorption capacities at inflow and outflow concentrations. Preferential flow paths can additionally contribute to the broadening of the breakthrough curves. Our breakthrough curves for P and As with 1000 μg L^{-1} inflow concentrations were relatively sharp and the estimated number of treatable BVs was in the range of adsorption capacities estimated from inflow concentrations. This indicates that adsorption equilibrium was largely reached and that preferential flow paths in the columns were not important.

4.2. Column breakthrough curves

Fibrils made from β-lactoglobulin (178 amino acids and a molecular weight of 19.883 Da) can enter the macropores of the activated carbon with a size of 2–4 μm (Fig. 1A–D), but not transitional pores (effective radii of 40–200 Å) and micropores (18–20 Å).[24] With the active phase of the sorbent located mostly on the surface and in macropores, we expect that intraparticle diffusion is of minor importance for As-removal by the fibrils and that the rate of reaching equilibrium is mostly defined by film diffusion and the rate of adsorption within the protein.

The kinetic fits to the data of the batch experiments show that the adsorption of As in suspended adsorbent can be described well by a second-order rate law of a one-site Langmuir model. The simplest model to describe

corresponding breakthrough curves in columns, assuming Langmuir-type adsorption, is the Thomas model. With the approximation of a rectangular adsorption isotherm, the Thomas equation reduces to the equivalent Bohart–Adams equation.[25] We used the expression as given by Trgo[26] and Hashim:[27]

$$\frac{c}{c_0} = \frac{1}{1 + \exp\left[\frac{k_{Th}}{Q} \cdot (q \cdot m - c_0 \cdot V)\right]} \quad (5)$$

Where k_{Th} is the Thomas rate coefficient, and in our RSSCTs, Q was the flow rate in (L h^{-1}), q the adsorption capacity of the adsorbent (μg mg^{-1}), m the mass of the adsorbent (mg), c_0 the inflow concentration (μg L^{-1}) and V the filtered volume (L).

As shown in Fig. 5 and 6, the breakthrough curves can be explained reasonably well by the Thomas equation. With values for k_{Th} and q (Table 3), optimized with the solver function in Excel, the maximum capacities q are similar to the capacities (C_{max}) estimated for As(v) of 10.5 and 16.2 μg mg^{-1} from the batch adsorption kinetics and the equilibrium Langmuir isotherm (Table 2). They are higher than the capacities determined for equilibrium with 10 μg L^{-1}, because the adsorbent at the inlet of the column is in contact with the high inflow concentration. Also, over the overall much longer time of interaction in the column, the protein fibrils can possibly accommodate more As than in the shorter batch experiments.

We did not attempt to find a relation between the kinetic Langmuir rate coefficients for adsorption and desorption and the Thomas rate coefficient, because the flow conditions and packing of the solid phase were different in the batch and the column experiments. A more detailed modeling of adsorption isotherms and breakthroughs was not the goal of these first columns studies with this novel adsorbent. The main objective was to determine achievable BVs, until effluent concentrations reached 10 μg L^{-1}. Our breakthrough curves for arsenate and phosphate are sharper than those reported for granular ferric hydroxide (GFH)[28] and we did thus not model the results with HSDM models,[28] applied by other authors for iron(hydr)oxide adsorbents. In these adsorbents, intraparticle diffusion was important and resulted in broader breakthrough curves than observed in our columns. To model the breakthrough curves with GFH, the homogeneous surface diffusion model (HSDM) with

Table 3 Parameters[a] of fits with the Thomas equation

Thomas equation	k_{Th} As μg^{-1} L h^{-1}	k_{Th} P μg^{-1} L h^{-1}	$q(C_{max})$ As μg mg^{-1}	$Q(C_{max})$P μg mg^{-1}
As(v) 100 μg L^{-1}	$4.9 \pm 1.1 \times 10^{-5}$		9.0 ± 1.0	
As(iii) + P 1000 μg L^{-1}	$1.4 \pm 0.5 \times 10^{-5}$	$2.0 \pm 0.6 \times 10^{-5}$	12.1 ± 1.0	9.3 ± 1.0
As(v) + P 1000 μg L^{-1}	$1.6 \pm 0.5 \times 10^{-5}$	$2.7 \pm 0.8 \times 10^{-5}$	11.4 ± 1.0	8.5 ± 1.0

[a] Error ranges were estimated by variation of the parameters around the optimal values until the sum of squared differences between measured and fitted data points increased by 20% or more, and the fits were visibly outside most of the data points.

382 | Environ. Sci.: Water Res. Technol., 2023, **9**, 375–385

This journal is © The Royal Society of Chemistry 2023

Freundlich isotherms was applied, using the Fixed-bed Adsorption Simulation Tool (FAST 2.0).[28,29]

4.3. Number of treatable BVs compared to other adsorbents

Due to their importance for As-removal in practice, iron(hydr)oxide-based adsorbents were studied by several groups. Driehaus[30] investigated treatment capacities of GFH as a function of initial As-concentrations, pH and other parameters. Treatment capacities increased with decreasing As inflow concentrations and decreased with increasing pH. At inflow concentrations from 10–30 $\mu g\ L^{-1}$, treatment capacities were between 50 000–300 000 BVs, with a large scatter in plots showing the relationship between inflow concentration and treatment capacity (due to differences in pH values and concentrations of other ions in the different source waters). On average, there was an approximately four-fold decrease of BVs with increasing pH from 7.0–8.0 (contact times of 3–10 minutes).

In RSSCTs with GFH and inflow concentrations in tap water (pH 7.6), spiked with 500 $\mu g\ L^{-1}$ As(III) and As(v) (without added phosphate and unspecified P-concentrations), Thirunavukkarasu et al.,[31] obtained 3240 and 3000 BVs, respectively. Also in RSSCTs with GFH, Westerhoff et al.[32] found that for groundwaters with influent arsenic concentrations of 14 $\mu g\ L^{-1}$ to 51 $\mu g\ L^{-1}$, 25 000 to 50 000 BVs could be treated before effluent arsenic concentrations exceeded 10 $\mu g\ L^{-1}$. Corresponding adsorption densities were 0.06 to 0.28 mg As/g GFH. In spiked synthetic groundwater with an influent of 100 $\mu g\ L^{-1}$, ca. 12 000 BVs could be treated to below 10 $\mu g\ L^{-1}$.[32] With a mesoporous hybrid material of thiol-functionalized silica-coated activated alumina, Hao et al.[33] achieved 3100 BVs with 70 $\mu g\ L^{-1}$ As inflow concentration (80% as As(III)) and a pH value of 7.3 in field column tests. Kanematsu et al.[34] investigated the effect of pH, silicate and phosphate on As-removal with a nanostructured goethite-based granular porous adsorbent (Bayoxide E33), and achieved up to ca. 68 000 BVs at pH 7.0 and 42 000 BVs at pH 8.3 with 120 $\mu g\ L^{-1}$ inflow As(v). Tresintsi et al. (2013)[35] reported 20 000 BVs for GFH and 24 000 BVs for E33 with water (pH 7.3) with 100 $\mu g\ L^{-1}$ As(v), 0.3 mg L^{-1} PO_4, 20 mg L^{-1} SiO_2, 360 mg L^{-1} HCO_3^-, and adsorption capacities of 3.4 $\mu g\ mg^{-1}$ Fe for GEH and 9.1 $\mu g\ mg^{-1}$ Fe for E33 in RSSCT experiments. These authors point out that much higher capacities can be reached by precipitation/coagulation, but that small-scale treatment is more convenient with fixed be adsorption columns. Tresintsi et al. (2012)[36] also report synthesis of a Schwertmannite phase adsorbent with high capacities of 13 μg As(v)/mg and 1.5 μg As(III)/mg at 10 μg As/L equilibrium concentration in National Sanitation Foundation test water with 100 μg As/L at pH 7. A comparison of RSSCT capacities is provided in Table 4.

The number BVs in our RSSCTs with spiked tap water with 100 $\mu g\ L^{-1}$ As(III) and As(v) of 68 000 at pH 7.5–8.0 were higher than values reported for Bayoxide E33 and higher than for

Table 4 Comparison of RSSCT capacities

Adsorbent	RSSCT capacities ($\mu g\ mg^{-1}$)	
	As(III)	As(v)
Nanofibril–carbon (100 $\mu g\ L^{-1}$ As)	>6.2	6.8
Nanofibril–carbon (1.0 $\mu g\ L^{-1}$ As + P)	5.8	6.0
pH 4 Schwertmannite precipitate[36]	5.7	15.0 (8.4[a])
pH 5.5 precipitate[36]	5.1	8.8
GFH (akaganeite)[36]	1.7	3.1
GFO Bayoxide (goethite)[36]	2.6	6.1

RSSCT capacities for 10 $\mu g\ L^{-1}$ effluent concentrations of the nanofibril–carbon composite (influent concentrations in parentheses) and of adsorbents listed in Tresinsti et al. (2012), in their Table 3 and Fig. 12[a], with influent concentrations of 100 $\mu g\ L^{-1}$ for As(V) and 250 $\mu g\ L^{-1}$ for As(III).[36]

GFH reported under similar conditions (see references above). Importantly, breakthrough with As(III) in the feed water did not occur earlier than for As(v). As(III) is generally oxidized to the better sorbing As(v) before removal in fixed-bed columns. Our adsorption isotherms show that As(III) was adsorbed as well as As(v) by the protein fibrils, although the sorption capacity for As(III) in the batch experiments was lower than for As(v). In the columns, sorbed As(III) is most likely oxidized to As(v) within days under the aerobic conditions employed and As(III) and As(v) re-distribute between As(III)-binding As(v)-binding sites. We did not attempt yet to determine the As oxidation state in the columns. The important result of this study is that columns with the protein fibril-activated carbon adsorbent can remove both As(III) and As(v) without pre-oxidation of As(III).

4.4. Possible (ad)sorption mechanisms

The mechanisms for the sorption of As and P in the amyloid fibrils are still unknown. As reported, proteins acting as ion channels on cell surfaces can bind arsenate and phosphate, some of them with high selectivity for As(v) or P.[37–39] To investigate the possible roles of amino acid residues in the binding of arsenite and arsenate, Bolisetty et al. performed in silico protein-chemical docking analysis on the binding of arsenite and arsenate to the β-lactoglobulin protein monomer. As(III) has a high binding affinity towards thiol groups and binds easily to cysteine residues of proteins, and there also sites for specific binding of arsenate.[12,40]

4.5. Leaching experiments and compliance with food safety

Leaching experiments were conducted by TÜV Rheinland Italia S.r.l., according to test protocol EN 1186, determining if the new and used adsorbent (until the outflow exceeded 10 $\mu g\ L^{-1}$) is safe in contact with food and drinking water. The material did not leach any dangerous substance including arsenic into the water and did not change the organoleptic properties of water as per EU Regulation 1935/2004 Article 3. Leaching tests according to the EN 12457 (European Union) and TCPL (US) protocols still have to be conducted.

5. Conclusions

The investigated novel protein-fibril active-carbon composite is highly effective in removing both As(III) and As(V) and a range of toxic elements from drinking water. The numbers of BVs reached in our RSSCT experiments for the removal of arsenic from water with typical ranges of ions were equal or higher than those reported for the most widely used adsorbents, for example for GFH and Bayoxide, when tested under similar conditions. For inflow concentrations of 100 μg L^{-1} As(III) and As(V), which covers As-concentrations in typical water sources used for drinking water, up to 68 000 BVs could be reached before outflow concentrations rose to above 10 μg L^{-1}. During the first 40 000 BVs, outflow concentrations for As were lower than 1 μg L^{-1}, which is relevant for water treatment in countries where lower limits will be enforced. To predict achievable BVs for inflow concentration below 100 μg L^{-1}, more tests will be needed, but judging from the roughly linear relationship observed with 100 μg L^{-1} and 1000 μg L^{-1} As, more than 120 000 BVs might be expected for inflow concentrations lower than 50 μg L^{-1}. The cost to treat the tested water with 50–100 μg As/L would be 0.05–0.1 Euro per m^3. Distinct advantages of the new sorbent over the currently used iron(hydr)oxide-based adsorbents are: (i) pre-oxidation of As(III) is not necessary; (ii) a range of other unwanted ions are also removed efficiently; (iii) ions normally present and considered beneficial in water used for drinking are not removed; (iv) the adsorbent is partially regenerable by flushing with dilute base (10 mM NaOH). Adaptation of the adsorbent into larger aggregated particles and other tests for upscaling to larger columns are in progress. The protein fibril adsorbents remove arsenic and other ions according to yet not well defined, but very different mechanisms than the well-investigated adsorption mechanisms on metal(hydr)oxide adsorbents. These novel adsorbents are thus a valuable addition to the established adsorbents, with a range of potentially important advantages in many situations.

Conflicts of interest

Sreenath Bolisetty has patent #EP2921216A1 licensed to Sreenath Bolisetty. SB and AR are the inventors of the two related patents (EP2921216A1 and US 63065824) filed on behalf of ETH Zurich and BluAct Technologies GmbH. Sreenath Bolisetty reports is cofounder of BluAct technologies GmbH.

Acknowledgements

References

1 S. Murcott, *Arsenic Contamination in the World, An International Sourcebook 2012*, IWA Publishing, 2012.

2 J. Podgorski and M. Berg, Global threat of arsenic in groundwater, *Science*, 2020, **368**, 845–850.

3 S. J. Hug, L. H. E. Winkel, A. Voegelin, M. Berg and A. C. Johnson, Arsenic and Other Geogenic Contaminants in Groundwater-A Global Challenge, *Chimia*, 2020, **74**, 524–537.

4 D. Mohan and C. U. Pittman Jr, Arsenic removal from water/wastewater using adsorbents-A critical review, *J. Hazard. Mater.*, 2007, **142**, 1–53.

5 J. G. Hering, I. A. Katsoyiannis, G. A. Theoduloz, M. Berg and S. J. Hug, Arsenic removal from drinking water: Experiences with technologies and constraints in practice, *J. Environ. Eng.*, 2017, **143**, 03117002.

6 D. Van Halem, S. A. Bakker, G. L. Amy and J. C. Van Dijk, Arsenic in drinking water: A worldwide water quality concern for water supply companies, *Drinking Water Eng. Sci.*, 2009, **2**, 29–34.

7 S. Y. Lu, H. M. Zhang, S. O. Sojinu, G. H. Liu, J. Q. Zhang and H. G. Ni, Trace elements contamination and human health risk assessment in drinking water from Shenzhen, China, *Environ. Monit. Assess.*, 2015, **187**, 4220.

8 Z. Abbas, M. Imran, N. Natasha, B. Murtaza, M. Amjad, N. S. Shah, Z. U. H. Khan, I. Ahmad and S. Ahmad, Distribution and health risk assessment of trace elements in ground/surface water of Kot Addu, Punjab, Pakistan: a multivariate analysis, *Environ. Monit. Assess.*, 2021, **193**, 351.

9 P. Singh, A. Borthakur, R. Singh, R. Bhadouria, V. K. Singh and P. Devi, A critical review on the research trends and emerging technologies for arsenic decontamination from water, *Groundw. Sustain. Dev.*, 2021, **14**, 100607.

10 S. Bolisetty and R. Mezzenga, Amyloid-carbon hybrid membranes for universal water purification, *Nat. Nanotechnol.*, 2016, **11**, 365–371.

11 S. Bolisetty, M. Peydayesh and R. Mezzenga, Sustainable technologies for water purification from heavy metals: review and analysis, *Chem. Soc. Rev.*, 2019, **48**, 463–487.

12 S. Bolisetty, N. Reinhold, C. Zeder, M. N. Orozco and R. Mezzenga, Efficient purification of arsenic-contaminated water using amyloid-carbon hybrid membranes, *Chem. Commun.*, 2017, **53**, 5714–5717.

13 Q. Zhang, S. Bolisetty, Y. Cao, S. Handschin, J. Adamcik, Q. Peng and R. Mezzenga, Selective and Efficient Removal of Fluoride from Water: In Situ Engineered Amyloid Fibril/ZrO2 Hybrid Membranes, *Angew. Chem., Int. Ed.*, 2019, **58**, 6012–6016.

14 M. Peydayesh, M. Pauchard, S. Bolisetty, F. Stellacci and R. Mezzenga, Ubiquitous aluminium contamination in water and amyloid hybrid membranes as a sustainable possible solution, *Chem. Commun.*, 2019, **55**, 11143–11146.

15 M. Peydayesh and R. Mezzenga, Protein nanofibrils for next generation sustainable water purification, *Nat. Commun.*, 2021, **12**, 3248.

384 | *Environ. Sci.: Water Res. Technol.*, 2023, **9**, 375–385

This journal is © The Royal Society of Chemistry 2023

16 F. Yang, Q. Yang, M. Chen, C. Luo, W. Chen and P. Yang, Toxic metal ion sequestration by amyloid-mediated fast coacervation, *Cell Rep. Phys. Sci.*, 2021, **2**, 100379.

17 Q. Zhang, S. Zhang, Z. Zhao, M. Liu, X. Yin, Y. Zhou, Y. Wu and Q. Peng, Highly effective lead (II) removal by sustainable alkaline activated β-lactoglobulin nanofibrils from whey protein, *J. Cleaner Prod.*, 2020, **255**, 120297.

18 S. Bolisetty, N. M. Coray, A. Palika, G. A. Prenosil and R. Mezzenga, Amyloid hybrid membranes for removal of clinical and nuclear radioactive wastewater, *Environ. Sci.: Water Res. Technol.*, 2020, **6**, 3249–3254.

19 M. Peydayesh, M. K. Suter, S. Bolisetty, S. Boulos, S. Handschin, L. Nyström and R. Mezzenga, Amyloid Fibrils Aerogel for Sustainable Removal of Organic Contaminants from Water, *Adv. Mater.*, 2020, **32**, 1907932.

20 S. Bolisetty, R. Mezzenga and A. Rahimi, Arsenic removal from Peruvian drinking water using milk protein nanofibril–carbon filters: a field study, *Environ. Sci.: Water Res. Technol.*, 2021, **7**, 2223–2230.

21 S. M. Loveday, S. G. Anema and H. Singh, β-Lactoglobulin nanofibrils: The long and the short of it, *Int. Dairy J.*, 2017, **67**, 35–45.

22 S. Bolisetty and R. Mezzenga, Composite material used in filter for water treatment and recovery of metals, comprises amyloid fibrils and activated carbon in intimate contact, and optionally support material, EP2921216A1, WO2015140074A1, 2015.

23 M. Usman, I. Katsoyiannis, J. H. Rodrigues and M. Ernst, Arsenate removal from drinking water using by-products from conventional iron oxyhydroxides production as adsorbents coupled with submerged microfiltration unit, *Environ. Sci. Pollut. Res.*, 2021, **28**, 59063–59075.

24 M. M. Dubinin and P. L. Walker, *Chemistry and Physics of Carbon*, Marcel Dekker, New York, 1966.

25 K. H. Chu, Fixed bed sorption: Setting the record straight on the Bohart-Adams and Thomas models, *J. Hazard. Mater.*, 2010, **177**, 1006–1012.

26 M. Trgo, N. V. Medvidović and J. Perić, Application of mathematical empirical models to dynamic removal of lead on natural zeolite clinoptilolite in a fixed bed column, *Indian J. Chem. Technol.*, 2011, **18**, 123–131.

27 M. A. Hashim and K. H. Chu, Prediction of protein breakthrough behavior using simplified analytical solutions, *Sep. Purif. Technol.*, 2007, **53**, 189–197.

28 A. Sperlich, S. Schimmelpfennig, B. Baumgarten, A. Genz, G. Amy, E. Worch and M. Jekel, Predicting anion breakthrough in granular ferric hydroxide (GFH) adsorption filters, *Water Res.*, 2008, **42**, 2073–2082.

29 A. Dabizha, C. Bahr and M. Kersten, Predicting breakthrough of vanadium in fixed-bed absorbent columns with complex groundwater chemistries: A multi-component granular ferric hydroxide–vanadate–arsenate–phosphate –silicic acid system, *Water Res.: X*, 2020, **9**, 100061.

30 W. Driehaus, Arsenic removal – Experience with the GEH® process in Germany, *Water Sci. Technol.: Water Supply*, 2002, **2**, 275–280.

31 O. S. Thirunavukkarasu, T. Viraraghavan and K. S. Subramanian, Arsenic removal from drinking water using granular ferric hydroxide, *Water SA*, 2003, **29**, 161–170.

32 P. Westerhoff, D. Highfield, M. Badruzzaman and Y. Yoon, Rapid small-scale column tests for arsenate removal in iron oxide packed bed columns, *J. Environ. Eng.*, 2005, **131**, 262–271.

33 J. Hao, M. J. Han, C. Wang and X. Meng, Enhanced removal of arsenite from water by a mesoporous hybrid material – Thiol-functionalized silica coated activated alumina, *Microporous Mesoporous Mater.*, 2009, **124**, 1–7.

34 M. Kanematsu, T. M. Young, K. Fukushi, P. G. Green and J. L. Darby, Individual and combined effects of water quality and empty bed contact time on As(V) removal by a fixed-bed iron oxide adsorber: Implication for silicate precoating, *Water Res.*, 2012, **46**, 5061–5070.

35 S. Tresintsi, K. Simeonidis, A. Zouboulis and M. Mitrakas, Comparative study of As(V) removal by ferric coagulation and oxy-hydroxides adsorption: Laboratory and full-scale case studies, *Desalin. Water Treat.*, 2013, **51**, 2872–2880.

36 S. Tresintsi, K. Simeonidis, G. Vourlias, G. Stavropoulos and M. Mitrakas, Kilogram-scale synthesis of iron oxy-hydroxides with improved arsenic removal capacity: Study of Fe(II) oxidation-precipitation parameters, *Water Res.*, 2012, **46**, 5255–5267.

37 F. B. Hussein, K. Venkiteshwaran and B. K. Mayer, Cell surface-expression of the phosphate-binding protein PstS: System development, characterization, and evaluation for phosphorus removal and recovery, *J. Environ. Sci.*, 2020, **92**, 129–140.

38 K. Venkiteshwaran, E. Wells and B. K. Mayer, Kinetics, Affinity, Thermodynamics, and Selectivity of Phosphate Removal Using Immobilized Phosphate-Binding Proteins, *Environ. Sci. Technol.*, 2020, **54**, 10885–10894.

39 K. Venkiteshwaran, E. Wells and B. K. Mayer, Immobilized phosphate-binding protein can effectively discriminate against arsenate during phosphate adsorption and recovery, *Water Environ. Res.*, 2021, **93**, 1173–1178.

40 S. Shen, X. F. Li, W. R. Cullen, M. Weinfeld and X. C. Le, Arsenic binding to proteins, *Chem. Rev.*, 2013, **113**, 7769–7792.

This journal is © The Royal Society of Chemistry 2023

Environ. Sci.: Water Res. Technol., 2023, **9**, 375–385 | **385**